

Effect of the incorporation of gold nanoparticles on the current–voltage characteristics of Ag/Si diodes in the dark and under light

J. Ghabboun ^{a,*}, I. Musa ^b, N. Adawi ^a, M. Mousallam ^a

^a *Department of Sustainable Energy Engineering, Bethlehem University, Bethlehem, Palestine*

^b *Department of Physics, Palestine Technical University-Kadoorie, P. O. Box 7, Tulkarm, Palestine*

The use of nanoparticles in electronic devices has become common practice for controlling and improving device performance. In this research, gold nanoparticles (AuNPs) were introduced into silver–silicon (Ag/Si) Schottky diodes to investigate their impact on the current voltage (I–V) behavior in both the dark and light surroundings. Spin coating was used to deposit a film of AuNPs on the Si substrate, followed by thermal evaporation of Ag metal to create the concluding Ag/AuNP/Si diode. Study of the I–V curves revealed a reduction in the barrier height after the addition of AuNPs in both the dark and illuminated settings. Furthermore, the presence of AuNPs led to a decrease in both the series (R_s) and shunt (R_{sh}) resistances when the diode was exposed to light, indicating an improvement in the photosensitivity of the Ag/Si structures. This enhancement was attributed to the ability of AuNPs to increase light absorption through local interface plasmon excitations, resulting from the shared oscillation of free electrons on metallic surfaces.

(Received October 12, 2024; Accepted December 16, 2024)

Keywords: Silver–silicon junction, Gold nanoparticles, Schottky diode, Current–voltage, Barrier height

1. Introduction

The study of the effects of incorporating nanoparticles in metal–semiconductor devices is gaining momentum for increasing the use of such devices in electronics [1–3]. The effect of inserting Au-based nanomaterials in electronic devices has been extensively studied for novel optoelectronic applications, such as ultraviolet light emitters, thin film transistors, solar cells, sensors, transducers and biomedical applications [4,5]. Researchers have investigated methods to increase the performance of Schottky diodes by reducing the Schottky barrier height (Φ_b), series resistance (R_s), and trap energy, which directly impacts the development of Schottky diodes for optoelectronic applications [6].

The augmented attention in exploring the usage of gold nanoparticles (AuNPs) in novel performances is due to their unique physical and chemical properties. The addition of AuNPs to electronic devices is expected to enhance their optical properties owing to their surface Plasmon resonance special properties [7,8]. This optical phenomenon occurs when electromagnetic waves interact with a metal's conductive electrons such as the AuNPs. Owing to these exceptional optical phenomena and the chemical and electronic characteristics of AuNPs, scientists are attracted to developing specific technologies in the field of optoelectronics. These gold nanoparticles/rods are potentially used to connect elements of electronic chips [9,10]. Furthermore, AuNPs are considered preferable materials in various applications in nanoelectronics because of their detectability and compatibility with synthesis [11].

The changes made to the interface have a significant effect on the surface energy and defects, which in turn affects the chemistry and electronic structure of the systems being studied. These properties are crucial for understanding the behavior at different heterojunctions or heterointerfaces. Previous research by Djurišić et al. (2010) [12] and Jing et al. (2013) [13]

* Corresponding author: [jamalg@bethlehem.edu](mailto:jamal@bethlehem.edu)
<https://doi.org/10.15251/JOR.2024.206.879>

highlighted this. The main aim of this research is to carefully measure and analyze the electrical conduction characteristics of modified Si/Ag diodes with AuNPs. This investigation focuses specifically on analyzing essential parameters derived from a detailed analysis of current–voltage characteristics, such as the barrier height (Φ_b), the series and shunt resistances, in addition to other characteristics that define a nonideal Schottky diode [14].

2. Experimental

2.1. Ag/AuNP/Si diode preparation

The AuNPs were purchased from Sigma Aldrich in the form of a stabilized nanoparticle kept in a citrate buffer solution with a concentration of 0.1 mg/mL. The nanoparticles have a diameter of 10 nm and are kept at 2–8°C. The substrates of the silicon wafer were cut into 1 cm × 1 cm pieces and etched to remove defects and impurities. Etching process was carried out by dipping Si substrates in ethanol (CH₃CH₂OH, 95%) for thirty seconds, followed by plunging them in distilled water for another thirty seconds followed by immersion in a KOH (30% wt) solution [15]. They were then heated at 82°C on a hot plate to evaporate the solutions for 45 minutes. After being rinsed in DW and ethanol (95%), the samples were left to dry at room temperature. A total of 15 mL of AuNPs was dropped onto the Si substrate via a micropipette for deposition. The AuNPs were then coated on the Si substrate using a spin coater for a time of sixty seconds at a rate speed of 1200 rpm. Afore the thermal disposition of a thin metal layer of Ag, the sample was tested via Fourier-Transform infrared (FTIR) spectroscopy to demonstrate the effective coating of the nanoparticles. The thickness of the coated film declined as the coating speed rise [16, 17]. A thermal evaporator was used for Ag metal deposition [18]. Ag solid was placed in the crucible to be evaporated on top of the Si substrate. The evaporator chamber was evacuated to around 10⁻⁷ Torr. The tungsten holder that form the crucible is heated slowly by letting the current to drive through the two electrodes, causing the Ag contained in the crucible to evaporate and deposit on the Si substrates attached face down with the holder of the sample. The deposition ratio was adjusted to monitor a final thickness of approximately 100 nm.

3. Results and discussions

3.1. Fourier Transform Infrared of AuNPs/Si

Fourier transform infrared spectroscopy (FTIR) was used to confirm the successful deposition of the AuNPs on the etched Si substrate. A Bruker FTIR Routine Spectrometer (Billerica, MA, USA) was used to verify the deposition of AuNPs on the silicon substrates. The resultant spectrum was acquired using Opus 8.1 software and then processed through Origin2018 computational program [19]. Examination of the FTIR spectra revealed clear peaks that corresponded to the characteristic functional groups, indicating the presence of AuNPs encapsulated in carbonyl groups.

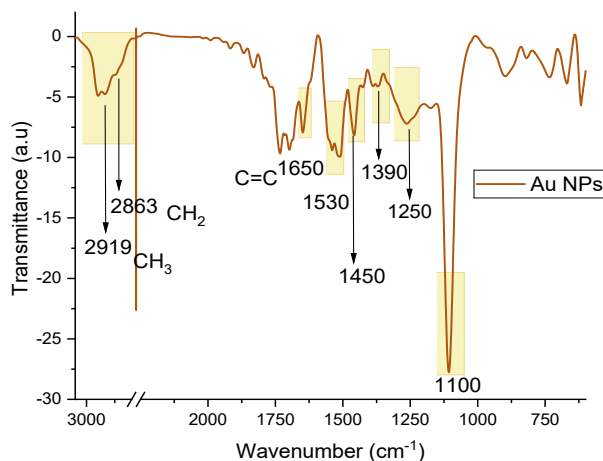


Fig. 1. Fourier-Transform Infra-Red spectrum of AuNPs in a citrate solution, peaks are labeled with their functional group.

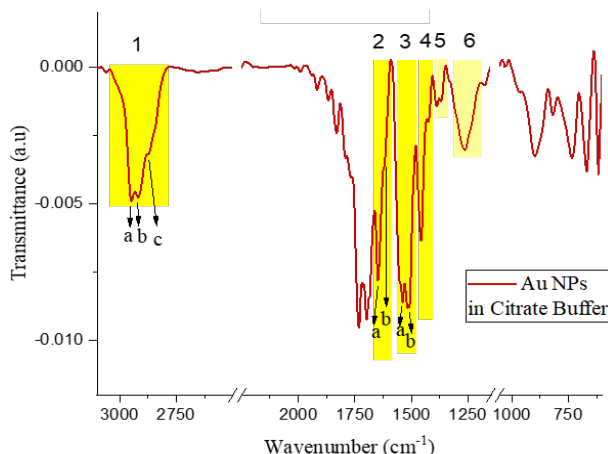


Fig. 2. Fourier-Transform Infra-Red spectrum of AuNPs on a Si substrate deposited with AuNPs in citrate buffer. Summary of labeled peaks are shown in Table 1.

Table 1. Main FTIR peaks for AuNPs in the Si substrate spectra depicted in Fig. 2.

Wavenumber (cm ⁻¹)	Functional Group (Vibrations)
1	(a) 2952 ν_{as} (stretching, asymmetric)CH ₃
	(b) 2922 ν_{as} (stretching, asymmetric)CH ₂
	(c) 2852 ν_s (stretching, asymmetric)CH ₃
2	(a) 1649.1 C = O carbonyl group symmetric stretching
	(b) 1619.8 C = O carbonyl group asymmetric stretching
3	1539 C – H Bending (asymmetrical)
	1511 Aromatic –C – C – groups
4	1458 δ (CH ₂) scissoring
5	(a) 1392.7 C – H Bending (symmetrical)
6	1265 Ester bond – representing the Citrate influence to the spectrum

Figure 1 displays only the FTIR spectrum for AuNPs, with results in line with those of previous reviews by Gurunathan et al. (2014) [20] and Moshfegh et al. (2011) [21]. The analysis revealed strong bonding between the functional groups and the Au, as indicated by the stretching in the band from 3000 to 2000 cm⁻¹. The FTIR spectrum of the AuNPs after deposition on Si, along with the important functional groups in Table 1, is shown in Figure 2. The FTIR spectra of the AuNPs illustrated in Fig. 2 revealed points at 1649.1 and 1619.8 cm⁻¹, which suggest the presence of two carbonyl C=O-related groups in the AuNPs, as stated by Moshfegh et al. (2011)[21]. The presence of CH groups in the AuNPs can also be attributed to the peaks at 2952, 2922, and 2852 cm⁻¹.

The FTIR analysis revealed peaks indicating the occurrence of carbonyl assemblies on the surfaces of the nanoparticles, but no distinct peaks for gold were observed. This finding is in agreement with a former study by Shakibaie and colleagues [22], which characterized gold nanoparticles produced by the aquatic microalga strain green *Tetraselmis*. Additionally, shifts in the FTIR peaks after the coating of the AuNPs on the silicon substrate designate the presence of AuNPs capped within groups such as carbonyls and C-H.

3.2. Atomic Force Microscopy

Atomic force microscopy (AFM) scanning of gold nanoparticles on a Si surface are shown in Figure 3. The surface in Fig. 3a is scanned at a size of 2.67 $\mu\text{m} \times 2.67 \mu\text{m}$. Figure 3b shows a 3-D topographies of the AuNPs, and Figure 3c shows the stripe profiles for the separated nanoparticles from image (a), revealing several sizes of Au nanoparticles (8 nm, 9nm and 21nm). Figure 3(d) shows a particle size distribution histogram for the AuNPs, which is based on data extracted from

approximately 1800 nanoparticles in the image in Figure 3a. An analysis via particle measurement software revealed that the average diameter of these nanoparticles was approximately 15 nm.

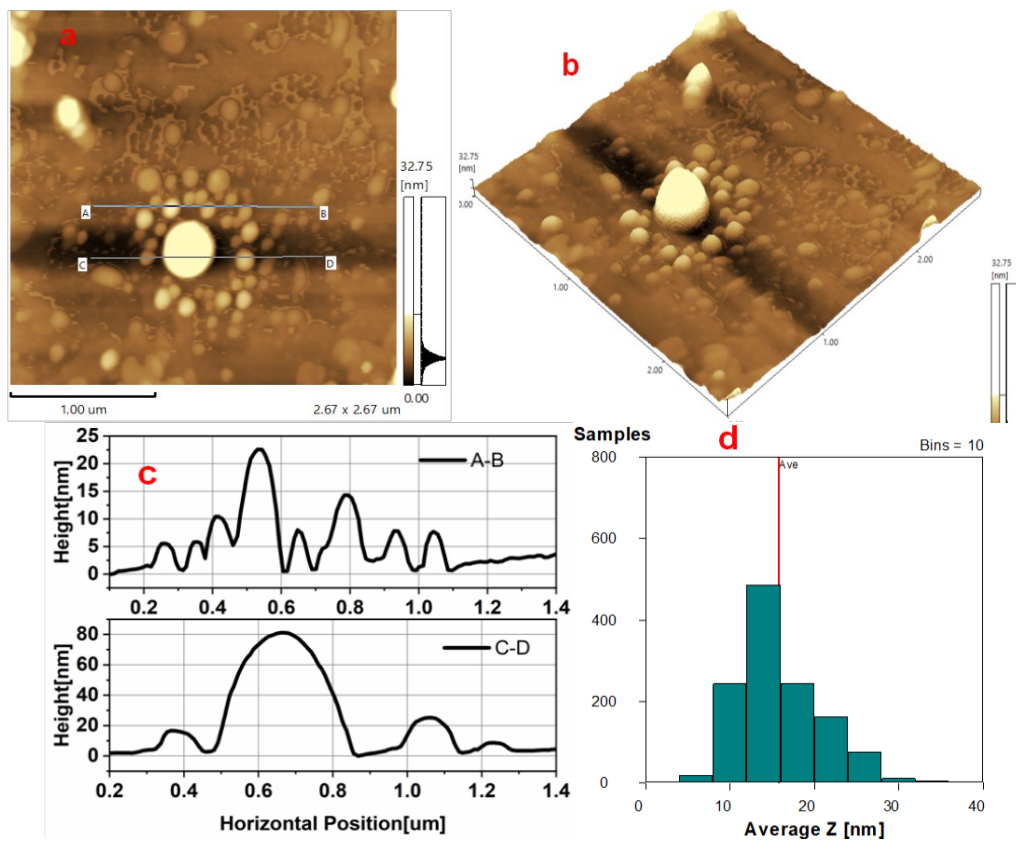


Fig. 3. (a) Atomic Force Microscopy images of AuNPs on a Si surface scanned at $2.67 \mu\text{m} \times 2.67 \mu\text{m}$. (b) 3-D projection of the AuNPs shown in (a). (c) Stripe profiles for separated AuNPs showing the sizes of the nanoparticles. (d) Particle size distribution histogram.

3.3. Current-voltage measurements

The Keithley 2601 source measurement unit (SMU) was utilized to perform DC voltage biasing and current measurements. This SMU instrument has the ability to measure both the precision voltage and current source in all four quadrants for both positive and negative voltages and currents. The electrical characterization circuit, illustrated in Figure 4, was constructed using micromanipulators for contacts. The circuit setup in Figure 4 included fabricated Au\NPs\Si diodes, with micromanipulators used for rear and upper contact to accomplish I–V curves. Ohmic top and back contacts were realized via silver paint, as depicted in Fig. 4.

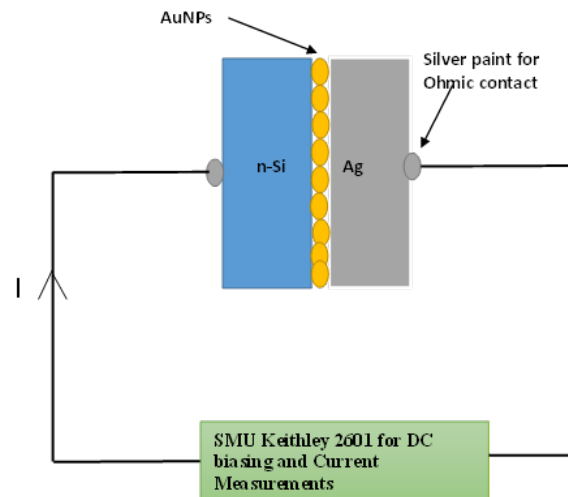


Fig. 4. Circuit setup for current–voltage measurements.

With the Keithley 2601 SMU, the fabricated diodes were tested across a range of -5 V to 5 V. Measurements were conducted on the Ag/Si and Ag/AuNPs/Si diodes to observe changes in their comportment in both dark and light shining environments to demonstrate the effects of illumination on the diodes' performance. The I–V results of Ag/AuNP/Si diode were then compared with measurements taken for Schottky diodes without AuNPs at the interface.

3.4. Effect of Light Illumination on Schottky Diodes

The impact of AuNPs on conductivity was examined by analyzing the produced I–V curve characteristics at both positive/negative biases. A single-diode comparable circuit model was used to fit the experimental data, as shown in Figure 5. This allowed for the estimation of the Schottky barrier height (Φ_b) and the series (R_s) and shunt (R_{sh}) resistances. Additionally, the influence of light effect on current–voltage characteristics was investigated. This was achieved by testing samples under both dark and light conditions. In other words, to study the effect of illumination induced current (I_{ph} : Photocurrent). The model used to fit the circuit containing the Ag/Si Schottky diode in Figure 5 includes shunt and series resistances, which impact the electrical behavior of the ideal diode model [23–26].

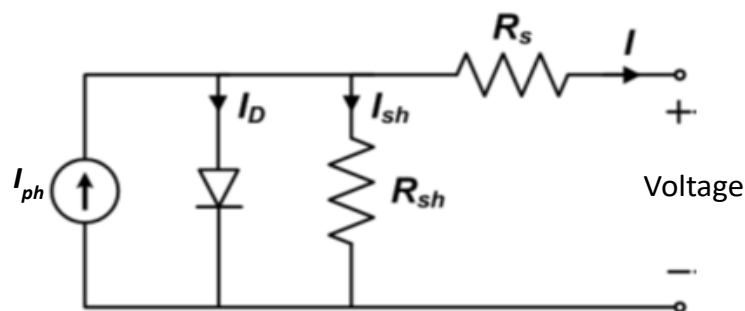


Fig. 5. Single Schottky diode model with shunt (R_{sh}) and series (R_s) resistances.

The I–V characterization curve factors were found to be lower than ideal, mainly because of the series resistance. Furthermore, the presence of shunt resistance was attributed to leakage across the metal–semiconductor junction from impurities and semiconductor defects within the depletion region [14]. The electric current circulating over the non-ideal Schottky diode relative to the input bias, as well as both the R_s and R_{sh} resistances, can be expressed via Equation (1) [27–30].

$$I = I_0 \left[\exp\left(\frac{V - R_s I}{nV_{th}}\right) - 1 \right] + \frac{V - R_s I}{R_{sh}} \quad (1)$$

where $V_{th} = \frac{k_B T}{q}$ is the thermal voltage, q is the electron charge, k_B is the Boltzmann constant, T is the absolute temperature, I_0 is the saturation current, V is the applied voltage and n is the ideality factor. This equation cannot be solved using analytical methods; consequently, the current's analysis and the computations of the factors of Φ_b , R_s and R_{sh} can be found via computer programs with a diode fitting mode analysis [27].

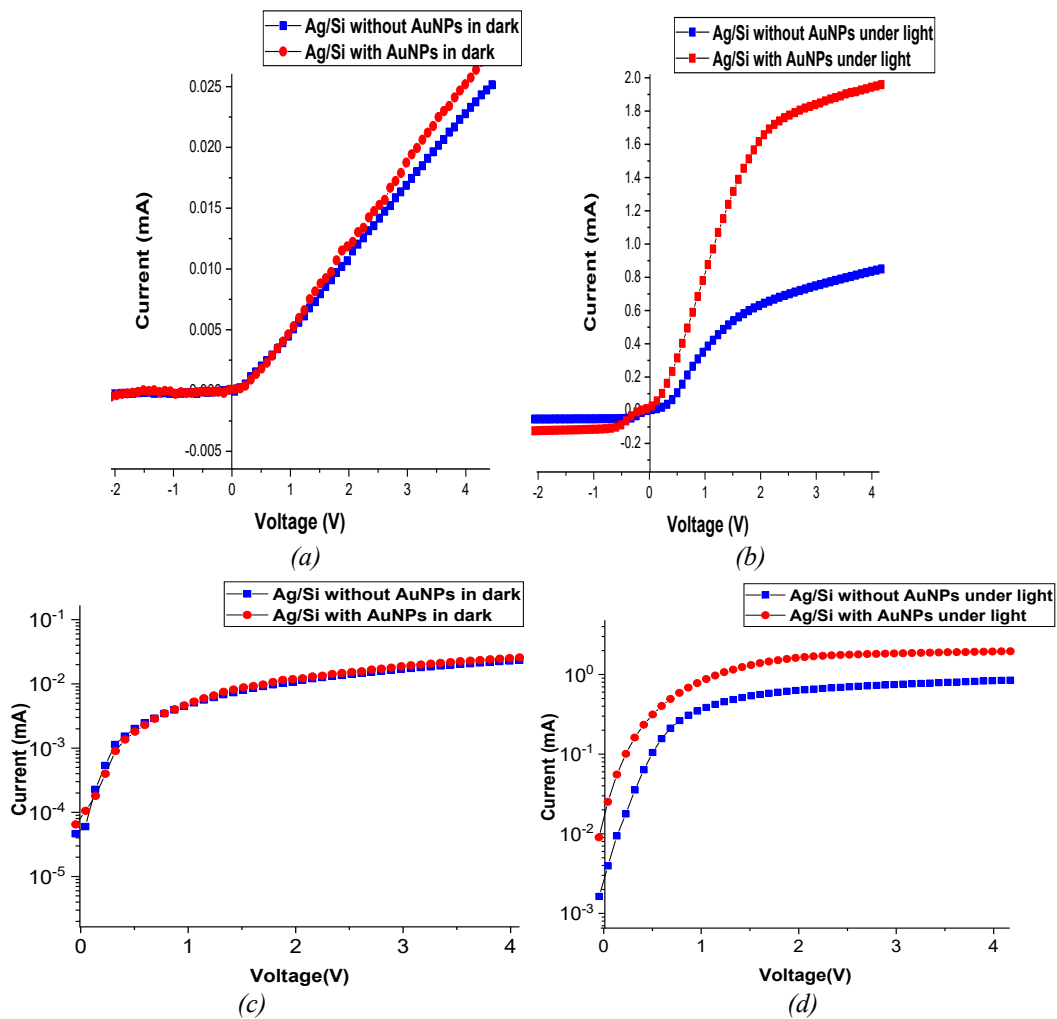


Fig. 6. (a) I - V characteristic curves of Ag/Si Schottky diodes with and without AuNPs in the dark. (b) I - V characteristic curves of irradiated Ag-Si diodes with and without AuNPs. (c) Logarithmic scale of I - V curves of forward voltage bias region for Ag-Si diodes with and without AuNPs in the dark. (d) Logarithmic scale of I - V curves of forward voltage bias region for Ag-Si diodes with and without AuNPs under illumination.

The experimental results and graphical representations of I-V measurements were analyzed, using Origin2018 (Origin Lab Co., Northampton, MA, USA) [19]. I-V curves were taken for the two types of made-up Schottky diodes, Ag/Si and Ag/AuNPs/Si, in the presence and absence (dark) of illumination, as shown in Figure 6, i.e., with a light directed at the diode during the measurement taken process. The Schottky diodes were exposed to illumination with an intensity of 1000 W/m^2 .

A logarithmic scale was used in the forward bias to clearly show the effect of AuNPs in the dark and under light on the current, as shown in Figure 6c and 6d.

Figure 6 shows the average I–V curves of the Ag/Si Schottky diodes with and without AuNPs in the dark and the average I–V curves of the same samples but with light exposure. Current-voltage measurements clearly indicate the rectification effect of diodes for Ag/Si and Ag/AuNPs/Si diodes in the dark and under illumination. The significant variance is the intensification in the current value by a factor of the order of 10^2 between the dark and light data, which can be elucidated by the reality that the illumination of the diodes with light resulted with a modification in the gap of energy, allowing the electrons at the Fermi level to transfer in a more efficient manner. The parameters R_s and R_{sh} and Φ_b were extracted respectively for each set and found by reiterating the same procedure in the investigation and calculation using ModDiode for fitting method constructed in Origin2018.

Table 2. Parameter values as influenced by the existence of AuNPs (a) in dark and (b) after irradiation.

(a) In Dark	Ag/Si	Ag/AuNPs/Si
I_o (A)	4.96×10^{-13}	1.41×10^{-07}
R_s (Ω)	82.75	117.28
R_{sh} (Ω)	4174.89	1752.47
Φ_b (V)	0.8	0.29
(b) exposed to light	Ag/Si	Ag/AuNPs/Si
I_o (A)	3.38×10^{-6}	3.09×10^{-4}
R_s (Ω)	1.99	1.17
R_{sh} (Ω)	18.06	16.37
Φ_b (V)	0.45	0.33

The results of the experiment demonstrate that the fabricated Ag/Si Schottky diodes, with and without AuNPs, are highly responsive to light and exhibit photovoltaic properties. When tested in the dark, the barrier height was found to be 0.8 V for Ag/Si, but this value decreased significantly to 0.29 V when AuNPs were added. Table 2 provides a comparison of the parameters obtained from the I–V characteristics in Figure 6, both in the dark and after illuminating the diodes. Importantly, the saturation current is approximately 6 times greater in order of magnitude, in the illuminated samples than samples tested in dark. Furthermore, the introduction of nanoparticles increased the current value in the forward bias, in both cases in the dark and under light. The series and shunt resistances were also much lower in the illuminated samples than in the dark samples. The results also revealed that the saturated current value increased with the addition of AuNPs, while the slightest amount of leak of the reverse bias region was observed in the dark measurements. These differences in the diode characteristics were evident in the I–V curves when tested in the dark. Additionally, the barrier height for bare Ag/Si decreased when illuminated, whereas it slightly increased for Ag/AuNPs/Si. The shunt resistance decreased significantly in the AuNP sample, whereas the series resistance increased. Both resistances decreased under light for both samples with and without AuNPs.

4. Conclusion

Research has shown that including gold nanoparticles (AuNPs) in Ag/Si Schottky diodes greatly improves their performance by decreasing the barrier height under both dark and light conditions. This decrease helps improve current conduction in the bulk area, which is crucial for the efficiency of the device. The presence of AuNPs also significantly lowers trap energy, reducing the barriers that block electron flow and further boosting the diode's function. Furthermore, the addition

of AuNPs has the potential to turn the Ag/Si diode into a highly efficient and advanced photovoltaic device, as seen from the remarkable increase in current when exposed to light.

The improved photosensitivity is exceptionally evident from the even lower series and shunt resistance under illuminated conditions than under dark conditions, indicating enhanced performance even under challenging lighting circumstances. Overall, incorporating AuNPs into Ag/Si diodes not only substantially improves their electrical properties but also greatly broadens the horizons for their utilization in innovative optoelectronic and cutting-edge photovoltaic applications. By incorporating AuNPs, Ag/Si diodes unlock tremendous potential for advancements in various technological fields, paving the way for exciting future developments and breakthroughs in the world of electronics.

Acknowledgments

The authors are thankful for the financial support from the Palestinian Ministry of Higher Education and Research, the fund was accorded through the Dean's Office of Research at Bethlehem University. Moreover, authors are appreciative to Palestine Technical University-Kadoorie (PTUK), for the Nano lab characterization and to Alquds University for the FTIR lab.

References

- [1] L. Amirav, M. Wächtler, Nano Schottky?, *Nano Lett.*, 22, (2022), 9783-9785; <https://doi.org/10.1021/acs.nanolett.2c04150>
- [2] B. Park, Chapter 1. Current and Future Applications of Nanotechnology, in: R.E. Hester, R.M. Harrison (Eds.), *Issues Environ. Sci. Technol.*, Royal Society of Chemistry, Cambridge, (2007), 1-18; <https://doi.org/10.1039/9781847557766-00001>
- [3] E. Guziewicz, I.A. Kowalik, M. Godlewski, K. Kopalko, V. Osinniy, A. Wójcik, S. Yatsunencko, E. Łusakowska, W. Paszkowicz, M. Guziewicz, Extremely low temperature growth of ZnO by atomic layer deposition, *J. Appl. Phys.*, 103, (2008), 033515; <https://doi.org/10.1063/1.2836819>
- [4] G. M. A. GAD and M. A. HEGAZY, "Optoelectronic properties of gold nanoparticles synthesized by using wet chemical method," *Mater. Res. Express*, 6 (8), 085024, IOP Publishing (2019); <https://doi.org/10.1088/2053-1591/ab1bb8>
- [5] S. Gravelins, M.J. Park, M. Niewczas, S.-K. Hyeong, S.-K. Lee, A. Ahmed, A.-A. Dhirani, *Commun. Chem.* 5, (2022), 1-10; <https://doi.org/10.1038/s42004-022-00723-2>
- [6] G.D.J. Smit, S. Rogge, T.M. Klapwijk, *Appl. Phys. Lett.* 80, (2002), 2568-2570; <https://doi.org/10.1063/1.1467980>
- [7] R. Liu, D. Zhan, D. Wang, C. Han, Q. Fu, H. Zhu, Z. Mao, Z.-Q. Liu, *Inorganics*, 11, (2023), 206; <https://doi.org/10.3390/inorganics11050206>
- [8] D.M. Schaadt, B. Feng, E.T. Yu, *Appl. Phys. Lett.*, 86, (2005), 063106; <https://doi.org/10.1063/1.1855423>
- [9] S. Chaudhary, S. Dangi, R. Singh, R. Chaudhary, *Int. J. Adv. Prod. Ind. Eng.*, 1(2),(2016), 45-50;
- [10] L. Sousa, L. Vilarinho, G. Ribeiro, A. Bogado, L. Dinelli, *R. Soc. Open Sci.*, 4, (2017), 170675; <https://doi.org/10.1098/rsos.170675>
- [11] R. Herizchi, E. Abbasi, M. Milani, A. Akbarzadeh, *Artif. Cells Nanomedicine Biotechnol.*, 44, (2016), 596-602; <https://doi.org/10.3109/21691401.2014.971807>
- [12] A.B. Djurišić, A.M.C. Ng, X.Y. Chen, *Prog. Quantum Electron.*, 34, (2010), 191-259; <https://doi.org/10.1016/j.pquantelec.2010.04.001>
- [13] L. Jing, W. Zhou, G. Tian, H. Fu, *Chem. Soc. Rev.*, 42, (2013), 9509-9549; <https://doi.org/10.1039/c3cs60176e>

- [14] M. Bashahu, D. Ngendabanyikwa, P. Nyandwi, *J. Mod. Phys.*, 13, (2022), 285-300; <https://doi.org/10.4236/jmp.2022.133020>
- [15] S. Franssila, *Introduction to Microfabrication*, 2nd edition, Wiley, Chichester, (2010); <https://doi.org/10.1002/9781119990413>
- [16] D.A. Ajadi, S.M. Agboola, O. Adedokun, *J. Mater. Sci. Chem. Eng.*, 4, (2016), 1-6; <https://doi.org/10.4236/msce.2016.45001>
- [17] S. Gorji, K. Razak, K.Y. Cheong, *J. Colloid Interface Sci.*, 408, (2013), 220-228; <https://doi.org/10.1016/j.jcis.2013.07.026>
- [18] M. M. Tavakoli, L. Gu, Y. Gao, C. Reckmeier, J. He, A.L. Rogach, Y. Yao, Z. Fan, *Sci. Rep.*, 5, (2015), 14083; <https://doi.org/10.1038/srep14083>
- [19] J.G. Moberly, M.T. Bernards, K.V. Waynant, *J. Cheminformatics*, 10, (2018), 5; <https://doi.org/10.1186/s13321-018-0259-x>
- [20] S. Gurunathan, J. Han, J. Park, J.-H. Kim, *Nanoscale Res. Lett.*, 9, (2014), 248; <https://doi.org/10.1186/1556-276X-9-248>
- [21] M. Moshfegh, H. Forootanfar, B. Zare, A.R. Shahverdi, G. Zarrini, M. Faramarzi, *Dig. J. Nanomater. Biostructures*, 6, (2011), 1419-1426;
- [22] M. Shakibaie, H. Forootanfar, K. Mollazadeh-Moghaddam, Z. Bagherzadeh, N. Nafissi-Varcheh, A.R. Shahverdi, M.A. Faramarzi, *Biotechnol. Appl. Biochem.*, 57, (2010), 71-75; <https://doi.org/10.1042/BA20100196>
- [23] E. Rodrigues, R. Melicio, V.M.F. Mendes, J. Catalão, *Proceedings of the International Conference on Renewable Energies and Power Quality - ICREPQ'11* 1(9), 2011, 369-373; <https://doi.org/10.24084/repqj09.339>
- [24] V. Tamrakar, S.C. Gupta, Y. Sawle, *Electr. Comput. Eng. Int. J.*, 4, (2015), 67-77; <https://doi.org/10.14810/ecij.2015.4207>
- [25] K. Thu, Y. Maung, *Int. J. Electron. Commun. Eng.*, 6, (2019), 5-9; <https://doi.org/10.14445/23488549/IJECE-V6I6P102>
- [26] K. Ukoima, E. Agwu, *Resistance, Umudike Journal of Engineering and Technology*, 5 (2019), 97-107; https://doi.org/10.33922/j.ujet_v5i1_11
- [27] S. Aazou, E.M. ASSAID, *IEEE*, (2010), 240; <https://doi.org/10.1109/ICM.2009.5418642>
- [28] S.M. Sze, ed., *Semiconductor sensors*, Wiley, New York, (1994).
- [29] S.S. Li, *Metal-Semiconductor Contacts*, in: S.S. Li (Ed.), *Semicond. Phys. Electron.*, Springer, New York, NY, (2006), 284-333; https://doi.org/10.1007/0-387-37766-2_10
- [30] R.L. Boylestad, L. Nashelsky, *Electronic Devices and Circuit Theory*, 10th ed., Prentice Hall Press, USA, (2008)